SENSOR TECHNIQUES TO VALIDATE THE STRESS INTENSITY IN CRACKED METALLIC PANELS REPAIRED WITH BONDED COMPOSITE PATCHES

Alan Baker and Bayram Aktepe
Airframes and Engines Division
Aeronautical and Maritime Research Laboratory,
Defence Science & Technology Organisation, Australia

SUMMARY: Design of bonded composite patch repairs for cracked metallic components is based on finite element or analytical models that determine the stress intensity ***K*** in the cracked component following patching and critical stresses in the patch system. To develop confidence in use of these models for the design of critical repairs there is a need to validate them experimentally.

In this paper a direct experimental approach is described in which ***K*** in a patched edge-notched specimen is measured using conventional strain gauges or special ***K***-gauges. Measurements were made at various crack lengths and over a range of temperatures. Generalized Westergaard equations with a rotated axis system were used to determine ***K*** from the strain measured using conventional gauges while an empirically derived equation was used for the ***K***-gauge.

These experimental results are encouraging since results for both types of gauges were in reasonable agreement with ***K*** predicted using the Rose or the Rose/Wang models.

KEYWORDS: Bonded Composite Repairs; Fatigue Crack Growth; Stress Intensity Factors

1 INTRODUCTION

Crack patching technology - repair of fatigue or stress corrosion cracked aluminium alloy airframe components with adhesively bonded advanced fibre composite reinforcements - pioneered in Australia since the mid 1970s has been extensively deployed on RAAF aircraft [1] and more recently on military aircraft in the US and Canada. These repairs based mainly on boron/epoxy patches and structural film adhesives, have proved to be highly efficient, durable and cost effective. There is thus incentive to develop a validated repair design capability to facilitate use in more demanding applications.

Design models to estimate the Mode1 stress intensity $\boldsymbol{K_I}$ in patched panels have been developed based on analytical or finite element approaches [2]. Initially to validate these models, studies were made to correlate the predicted ***K*** with observed fatigue crack growth behaviour, based on an assumed Paris-type relationship for crack growth rate. These studies were focused on Rose's analytical crack-patching model and fatigue results obtained from an edge-notched panel specimen [2,3].

Figure 1a) depicts the edge-notched specimen fatigue tested under constant load amplitude and Figure 1b) plots log ***da/dN*** versus log ΔK predicted using Rose's model [4], where ***a*** is the crack length ***N*** the number of cycles and ***K*** the stress intensity. These and other results [3] confirmed that this approach is a practical method for predicting ***DK*** in simple cracking geometries.

However, these fatigue experiments, whilst providing a useful validation of the models for practical application, are indirect, inaccurate (because of the use of log plots) and subject to the influence of several variables. There is a therefore a need to obtain a more direct validation of the models. Thus, as described in this paper, an experimental approach is described in which $\boldsymbol{K}$ is directly measured using either conventional strain gauges or special $\boldsymbol{K}$-gauges for a similar edge-notched specimen.

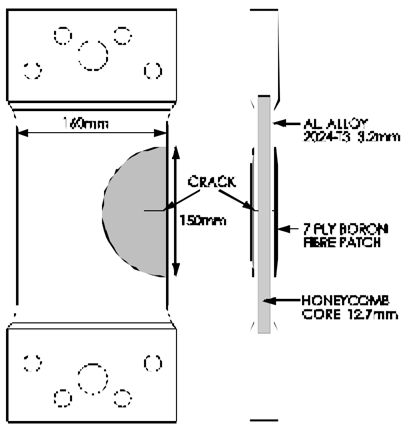

a)

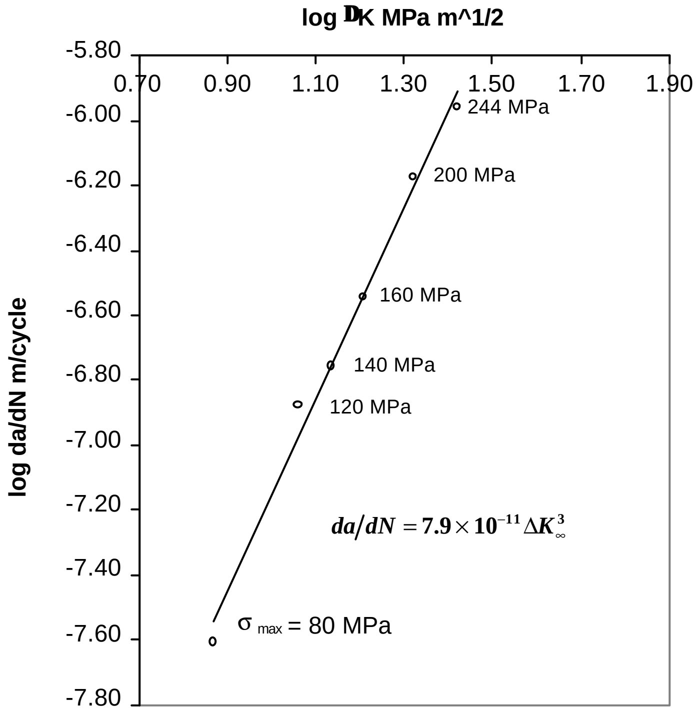

b)

Figure 1 *a) Generic structural detail test specimen for patched cracks in metallic structures used to validate the patching model and b) plot of experimental log* **da/dN** *versus log* $\boldsymbol{\Delta K}$*, obtained from Rose's analytical patching model.*

2 THE K-GAUGE

Based on the fact that the stress intensity factor can be obtained by measuring the stress distribution around a crack tip, a specially patterned foil strain gauge called the $\boldsymbol{K}$-gauge was developed by Kondo [5].

The $\boldsymbol{K}$-gauge consists of four grids concentrically located about the crack tip. The outer grid on either side of the crack has elements that are perpendicular to the crack line as shown in Figure 2. These are used to measure the average strain in the vertical direction and hence $\boldsymbol{K}_{\mathrm{I}}$. The inner grid on either side of the crack has elements which are parallel to the crack line and these measure the average strain in the horizontal direction and hence $\boldsymbol{K}_{\mathrm{II}}$.

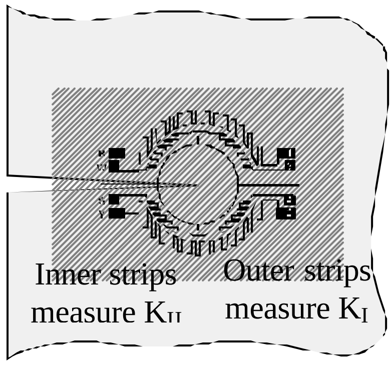

Figure 2: *Schematic diagram of the K gauge*

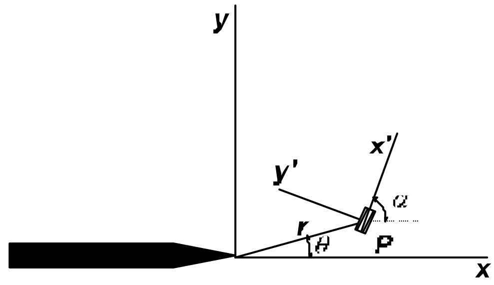

Figure 3: *Rotated axis system used for the strain-gauge approach.*

2.1 K-gauge Equations

As described by Miyake [6], the vertical elements of the ***K***-gauge are used to measure the Mode 1 stress intensity factor K_I, where the average strain is the elongation divided by the gauge element length. From the outer elements on either side of the crack tip, numbered 1 and 2, strains ε_1 and ε_2 are obtained which are related to K_I as follows:

$$K_I = c_1(\varepsilon_1 + \varepsilon_2) \tag{1}$$

The coefficient c_1 is derived empirically and is found to depend on the Young's modulus, E, and the Poisson's ratio, ν, of the material being used, and the crack length. Miyake has obtained values for this constant (shown in Table 1) for an aluminium alloy with a Young's modulus of 70.4 GPa and a Poisson's ratio of 0.3, hence these values of c_1 are used here.

a [mm]	c_1 [kg.mm$^{-1.5}$]
5	1.53
10	1.70
16	1.81
20	1.86
25	1.90
30	1.94

Table 1: *Values of* c_1 *for Equation 1 (for an aluminium alloy with* E *=70.4 GPa, and* ν *=0.3)*

3 THEORY OF K_I MEASUREMENT USING STRAIN GAUGES

3.1 Westergaard Equations

To enable the use of individual strain gauges, a mathematical relationship relating the strains to the stress intensity factor, is required. The relationship used here is obtained from the Westergaard equations [7] which are a suitable means of mathematically representing the strains in the vicinity of the crack tip.

It can be shown [8] that for a rotated coordinate system with strain gauges aligned at an angle α from the crack centreline, as shown in Figure 3, K_I may be expressed in terms of the product of the shear modulus, G, and the radial strain, $\varepsilon_{x'x'}$:

$$K_I = \sqrt{8r\pi}\, G\varepsilon_{x'x'} \left\{ \left(k - k^3\right)\sqrt{\frac{1}{1-k^2}} - \frac{1}{4}k\cos\left[5\tan^{-1}\left(\frac{k}{\sqrt{1-k^2}}\right)\right] + \frac{1}{4}\sqrt{1-k^2}\,\sin\left[5\tan^{-1}\left(\frac{k}{\sqrt{1-k^2}}\right)\right] \right\}^{-1} \tag{2}$$

$$\text{Where } k = \frac{1-\nu}{1+\nu} \tag{3}$$

For the 2024-T3 aluminium plate used in these experiments, the Young's Modulus E equals 72 GPa, the shear modulus G equals 27 GPa, and the Poisson's ratio ν is 1/3. Hence

$$k = \frac{1}{2} \quad \Rightarrow \quad K_I = \frac{16}{3}\sqrt{\frac{2\pi r}{3}}\, G\varepsilon_{x'x'} \tag{4}$$

and using the ratio of moduli for 2024-T3 Aluminium, $G/E = 3/8$, leads to the result:

$$K_I = \sqrt{\frac{8\pi r}{3}} E\varepsilon_{x'x'} \tag{5}$$

3.2 Rose's Inclusion Model for Stress Intensity

Very briefly Rose's model [4] is based on a two-stage analysis. In the first stage the reduction of stress caused by the patch or reinforcement bonded to an uncracked plate is estimated. The reinforcement is modeled as a stiff inclusion. In the second stage a semi-infinite crack is assumed to exist, fully covered by the reinforcement. The energy release rate G is then estimated for an incremental growth of the crack.

The net result is that the stress intensity in the patched structure is given by the equation:

$$K_R = \sigma_O \sqrt{\frac{\pi a \Lambda}{a + \Lambda}} \tag{6}$$

where

$$\pi\Lambda = \frac{1 + \frac{1}{S}}{\beta} \left(= \beta E_p t_p \frac{t_A}{G_A} \right) \qquad \text{[AB10](7)}$$

and

$$\beta^2 = \frac{G_A}{t_A} \left(\frac{1}{E_P t_P} + \frac{1}{E_R t_R} \right) \tag{8}$$

σ_0 is the reduced stress in the plate at the location of the crack, and is directly proportional to the applied stress. The constant of proportionality depends on the size, shape and elastic properties of the patch. S is the stiffness ratio of the patch to the plate, Λ is the characteristic crack length, and a is the crack length.

The upper bound for the stress intensity factor is given by the familiar equation:

$$K_\infty = \sigma_0 \sqrt{\pi \Lambda} \tag{9}$$

3.3 Wang's Crack bridging model:

A somewhat different approach to the analysis of repaired cracks under in-plane mixed mode loading was developed by Wang and Rose [9]. The model termed, the crack bridging model, is developed based on a characteristic spring constant, κ, that is a function of the shear transfer length, stiffness ratio and the Poisson's ratio.

The stress intensity factor of a reinforced plate as predicted by the crack bridging model is given by

$$K_R = \frac{\sigma_0}{\sqrt{\kappa}} \sqrt{\tanh \frac{\pi \kappa a}{1 + 0.345 \pi \kappa a}} \tag{10}$$

where the characteristic spring constant is given by

$$\kappa = \frac{1}{\pi\Lambda} \tag{11}$$

4 EXPERIMENTAL PROCEDURE

To determine whether the method of using individual strain gauges was applicable to this study, a number of static tests were conducted on unpatched 2024-T3 specimens with a crack length of 10mm. Since the stress intensity factor is jointly proportional to the square root of the distance and the radial strain, a number of strain gauges were radially placed at angles of 60°, as shown in Figure 4.

A suitable uniform strain region to place these gauges was determined using a thermal imaging technique [10]. The degree of undesirable curvature in the specimen was also examined using the same thermal imaging technique. Thermal scans of both sides revealed only a small curvature that could easily be tolerated.

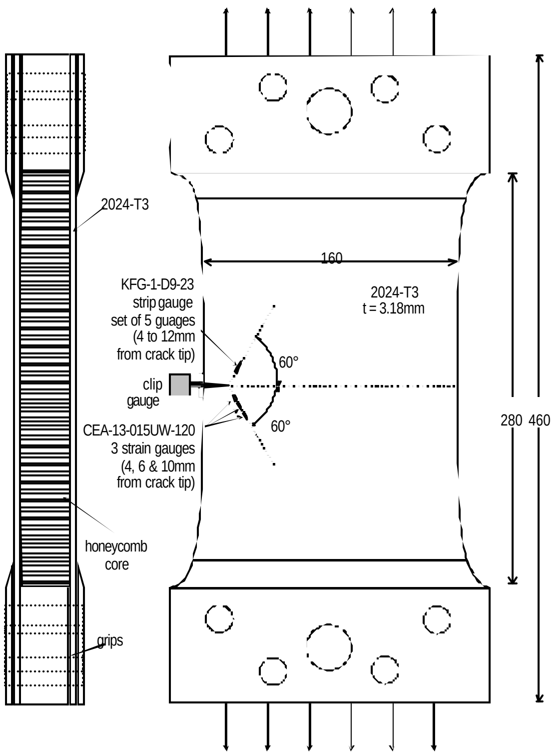

Figure 4: *Unpatched 2024-T3 specimen showing strain gauge locations for a crack with length a=10mm.*

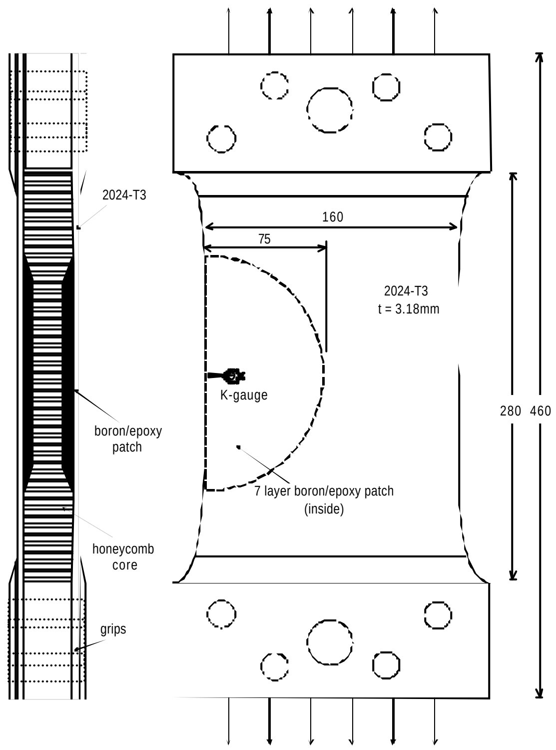

Figure 5: *Patched 2024-T3 specimen showing location of K-gauge for a crack with length a=10mm.*

The patched specimen used in the test program was a 2024-T3 specimen with the same dimensions as the previous unpatched specimen. Boron/epoxy patches of 150mm diameter were cocured with epoxy-nitrile film adhesive FM73 and then bonded using the same adhesive onto the inside face of each aluminium plate. Bonding of the patches to the inside allows the cracks to be monitored during fatigue cycling, while allowing the areas in the immediate vicinity of the crack tip to be instrumented. This patched specimen is shown in Figure 5.

The patches were bonded to the panels at the same time as the panels were bonded to the honeycomb core (i.e. cocured) a) to minimize curvature due to thermal expansion mismatch between the patch and b) to minimize the amount of secondary bending under load.

a) Testing was conducted on these specimens in the following combinations.
b) Unpatched specimen with crack length of 10mm
c) Patched specimen with crack length of 10mm

d) Unpatched specimen with crack length of 30mm

e) Patched specimen with crack length of 30mm

Static tests on the specimens for positive loads were conducted up to 80kN and for temperatures ranging from room temperature (20°C) up to 100°C.

The assumed properties of the materials and adhesive used in the experiments are shown in Table 2 and Table 3.

	t [mm]	***E*** [GPa]	***G*** [GPa]	***a*** [/°C]
2024-T3	3.14	72	27	$23x10^{-6}$
Boron/Epoxy	0.90	200	10	$4x10^{-6}$

Table 2: *Assumed properties of the materials (from [3])*

	Temperature			
Adhesive properties	20°C	60°C	80°C	100°C
G [GPa]	0.57	0.25	0.17	0.11
t [MPa]	36	16	12	8

Table 3: *Assumed properties of the adhesive (from [3])*

5 STRAIN SURVEYS

5.1 Unpatched Specimen

For the unpatched specimen with a crack length of 10mm, static tests were carried out at various temperatures, measuring radial strain at 60° to the crack centreline at a distance of 6mm from the crack tip. Stress intensity factors were calculated using equation 5. These results compared favourably with theoretical values calculated using the standard equation to determine ***K*** for an edge-crack [11] for an applied stress of 78.6 MPa. The results shown in Table 4 are in agreement with the theoretical value of 15.60 MPa√m, for a crack length of 10mm, to within 5%, as shown by the numbers in brackets in the table.

Temp °C	**Experimental K_I**
20	15.78 (1.2%)
40	15.65 (0.3%)
60	15.87 (1.7%)
80	16.27 (4.3%)

Table 4: *Stress intensity factors determined using a single strain gauge aligned at 60° on an unpatched specimen with gauges located 6 mm from the crack tip..*

These results demonstrate the validity of using a single strain gauge to determine the stress intensity factor for an unpatched specimen.

5.2 Patched Specimen

A patched specimen was also instrumented with a single strain gauge at 6 mm from the crack tip with a radial sensing direction along the 60° line to the crack tip. In addition a ***K***-gauge was bonded to this specimen with the centre of the gauge being placed directly over the crack tip. As for the unpatched specimen, tests were conducted at temperatures up to 80°C.

To enable comparison to be made with theoretical results, plots of experimental and theoretical results are shown in Figure 6.

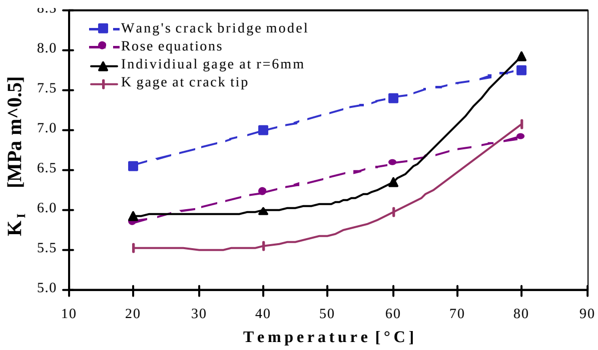

Figure 6: *Comparison of theoretical results for K_I from Rose's equations with measured values as a function of temperature (for* ***a****=10mm)*

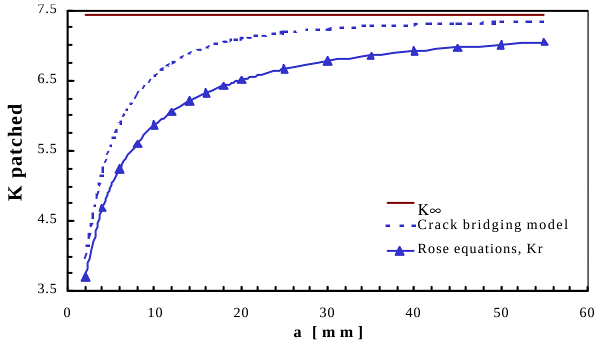

Figure 7: *Predicted variation of stress intensity K_1 with crack length at 20° C.*

This figure shows firstly that the shapes of the experimental curves differ from the theoretically predicted curves. While both Wang and Rose predict a more-or-less linear increase in ***K*** with temperature, experiment indicates the existence of a fairly strong parabolic relationship.

It can be seen that the estimate of ***K*** based on the Rose equations at the lower temperatures agreed (to within 10%) with measurements taken from both the individual strain gauge at 6mm from the crack tip and the ***K***-gauge. However, at high temperature (80°C), the individual strain gauge overestimated the theoretical ***K*** by 15%. It can also be seen that the ***K***-gauge underestimated theoretical values by up to 10% at the lower temperatures; however, it agreed well with the predictions at the high temperatures. Overall, considering the uncertainty in the adhesive properties used as input into the theoretical models, agreement with Rose's equations fairly reasonable.

The Rose/Wang crack bridging model [9] yields K_I values 12% higher than those predicted by the Rose equations for this crack length at ambient temperature so agrees quite well with the strain gauge result at the higher temperature.

6 CRACK LENGTH

Tests using only a ***K***-gauge were conducted on a patched specimen at a crack length of 30mm to check further the validity of the equations against the experimental results.

The predictions from the two models are shown in Figure 7. The upper-bound estimate K_∞ is quite good for crack lengths ***a*** above 30 mm, particularly for the Rose/Wang Model

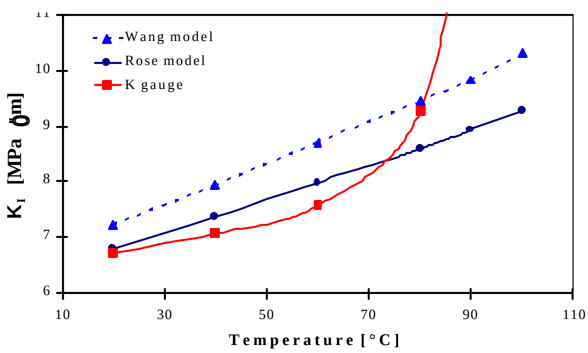

Figure 8: *Comparison of experimental and theoretical results for* ***K*** *for a=30mm, patched specimen.*

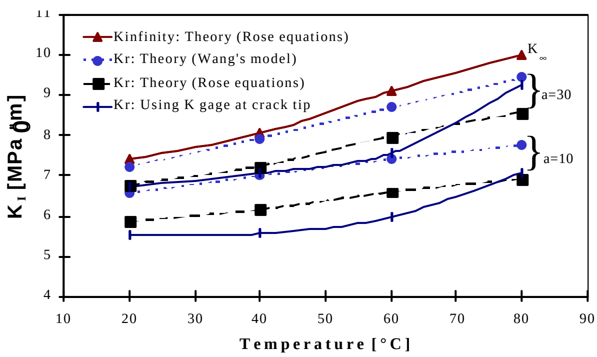

Figure 9: *Plots of* ***K*** *for a patched specimen for crack lengths of 10 and 30 mm, compared to predictions.*

The results obtained using the ***K***-gauge are shown in Table 5 and plotted in Figure 8. This figure shows that good agreement can be obtained with Rose's model at temperatures up to around 80°C at a = 30 mm. However, poor agreement is obtained at temperatures over 80°C where the patch is seen to become ineffective in reducing ***K***.

Temp [°C]	Theory (Rose)	Experiment	Relative difference
RT	6.78	6.72	-1%
40	7.24	7.07	-2%
60	7.99	7.57	-5%
80	8.59	9.27	8%
90	8.93	14.00	57%
100	9.27	21.05	127%

Table 5: *K_I measurements using a **K**-gauge, on a patched specimen with a=30mm. (Note the Wang model predicts K_I to be 8% higher than the Rose model for a=30mm.)*

Finally, for both crack lengths 10 and 30 mm, Figure 9 shows that the Rose equations agree quite well with the K-gauge measured ***K***, up to temperatures around 80°C.

Since the rate of crack growth, da/dN, in patched panels is proportional to the stress intensity factor, the sharp rise in the K around approximately 80°C is expected to lead to an acceleration in crack growth. This finding can be compared with fatigue results [3] that showed da/dN to increase only slightly at 80° C, but rapidly at 10° C, Figure 10.

7 TIME DEPENDANT BEHAVIOR

Further tests were conducted at temperatures between 80 and 100°C to investigate time-dependent behaviour on patching efficiency. As before, the patched specimen with the 30mm crack, the ***K***-gauge was used. Each channel of the ***K***-gauge and strain gauges was wired up to a data acquisition system and the sampling rate was set to 2 Hz. Strain data was recorded in applied stress increments of approximately 20 MPa up to 78.2 MPa.

The time dependency shown in at 80°C is for one channel of the ***K***-gauge, whereby the strain over a period of approximately 3 minutes increases by over 100%. This behaviour was seen on both channels measuring e_1 and e_2 and it results in an increase in ***K*** by around 10%.

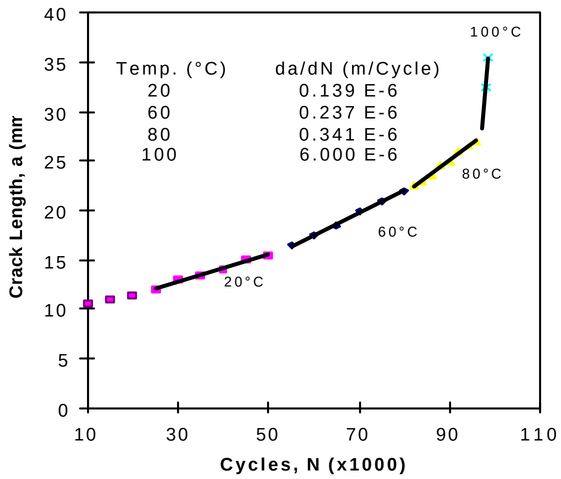

Figure 10: *Plot of crack length versus cycles at various temperatures, taken from* [3].

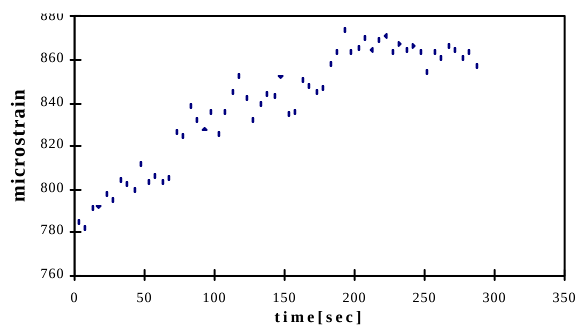

Figure 11: *Plot of strain versus time in a patched specimen with a 30mm crack length (at 80°C and 80kN).*

The time dependent behaviour observed is almost certainly associated with stress relaxation or creep of the FM73 adhesive even though short-term properties are reasonable at this temperature, Table 3.

This observation of time dependency explains the marked increase in K at 80° C, shown in Figure 11. However, as shown in Figure 10, the increase in K did not occur until 100° C for the fatigue test. The reason probably being that in the fatigue tests the strain rate was quite high, since load cycles were applied at around 3 Hz so the adhesive would have much less time to creep or relax than in the static tests. Building these time dependent effects into the patching models will be quite complex – the better approach being to use more creep resistant adhesives if significant loading of the repair occurs at elevated temperature.

8 CONCLUSIONS

The findings of this study may be summarized as follows:

Determination of K_I using single strain gauges: For the unpatched specimen it was found that with accurate placement and orientation of single strain gauges, K could be determined to within 5%.

Determination of K_I using K-gauge: For the patched specimen, the K-gauge K predictions were lower than those for the single gauge values by around 10%.

Comparisons with the patching models: The relationship for the measured K as a function of temperature differed from that predicted by the models. The models predicted a linear relationship whilst the observed relationship was parabolic. At the lower temperature, measured and predicted values of K agreed reasonably well - the measured values were generally closer to predictions by Rose's model. However, at elevated temperatures for the long crack the models did not predict the observed result. The differences between observed and predicted behaviour probably arise from inadequacies in the elevated temperature data for adhesive used in the analysis.

Time dependent behaviour of FM73 adhesive at elevated temperature: Significant time-dependent increases in K commenced at temperatures around 80°C. This is about 10°C lower than the fatigue test results had indicated. This observation indicates that creep or relaxation of the adhesive is much less at the higher frequency of loading used in the fatigue test, as would be expected from the rate dependent nature of the adhesive.

NOMENCLATURE

a	Crack length	Sub A	Adhesive
N	Cycles	Sub P	Panel
c_1	K-gauge strain coefficient	Sub R	Reinforcement or patch
E_p	Young's modulus of plate	r	Distance from crack tip to strain gauge
E_R	Young's modulus of reinforcement	S	Stiffness ratio of reinforcement to plate
G	Shear modulus	T	Temperature
k	Characteristic spring constant	t	Thickness
K	Stress intensity factor	a	Coefficient of thermal expansion
K_I	Mode 1 stress intensity factor	b	Reciprocal of the load transfer length
K_{∞}	Upper bound estimate of stress intensity factor	e	Strain
K_R	Stress Intensity following patching	L	Characteristic crack length
		n	Poisson's ratio
		s_0	Stress under the patch

REFERENCES

1 A.A. Baker, "Bonded Composite Repair of Metallic Aircraft Components", Paper 1 in AGARD-CP-550 Composite Repair of Military Aircraft Structures, 1994.

2 A.A Baker and R Jones,., (editors), "Bonded Repair of Aircraft Structures", Martinus Nijhoff Publishers, 1988.

3 A. A. Baker, "Fatigue Studies Related to Certification of Composite Crack Patching for Primary Metallic Structure" Proceedings of the FAA/NASA Symposium on Continued Airworthiness of Aircraft Structures, 1996, Atlanta USA.

4 L.R.F. Rose, "Theoretical Analysis of Crack Patching, " Chapter 6in Bonded Repair of Aircraft Structures, Editors A.A Baker and R Jones, Martinus Nijhoff, pp 107-173 1988.

5 Y..Kondo, "Stress Intensity Factor Measurement in Service Condition Using "K-gauge", VI International Congress on Experimental Mechanics, Portland, Oregon, June 6-10, 1988.

6 S. Miyake, Y. Nawa, Y.Kondo, & T. Endo, "Application of the "K-gauge" to Aircraft Structural Testing", Proceedings of ICAF, Jerusalem, 1989.

7 H. M Westergaard,, "Bearing Pressures and Cracks", Journal of Applied Mechanics, (1939) pp. A-49-53.

8 B. Aktepe and A. A. Baker (1998), "Experimental Estimation of the Stress Intensity In Cracked Metallic Panels Repaired With Bonded Composite Patches", Structural Integrity and Fracture, Edited by C. H. Wang, pp.1-12, Australian Fracture Group, ISBN: 0 646 360388.

9 C.H. Wang,. and L. R. F. Rose, "Bonded Repair of Cracks under Mixed Mode Loading", International Journal of Solids, **35** (1998), pp 2748-2773

10 T.G.Ryall, & A.K Wong,, "Design of a Focal-Plane Array Thermographic System for Stress Analysis", Experimental Mechanics, **35** (1995) pp144-147 June

11 D. Broek, "Elementary Engineering Fracture Mechanics", Martinus Nijhoff *Publishers*, Dordrecht, 1986